

NATIONAL TRANSPORTATION SAFETY BOARD

Office of Research and Engineering
Materials Laboratory Division
Washington, D.C. 20594



June 11, 2013

MATERIALS LABORATORY FACTUAL REPORT

Report No. 13-018

A. ACCIDENT INFORMATION

Place : Ellicott City, Maryland
Date : August 21, 2012
Vehicle : CSX Transportation coal train U183-18
NTSB No. : DCA12MR009
Investigator : Richard Hipkind, RPH-10

B. COMPONENTS EXAMINED

12 pieces of rail from the north rail.

C. DETAILS OF THE EXAMINATION

Overall views of the 12 submitted rail pieces are shown in figure 1. The pieces were from the north rail at the derailment site. The pieces were labeled N1, N5, N15A to N17A, N15B to N17B, N18, N19A and B, and N20. Based on the rail reconstruction conducted on-scene, the pieces were numbered with numbers increasing from west to east. The numbers were preceded by an N for the north rail. In cases where the rail was fractured in the web, the base portion was labeled with an A, and the head portion was labeled with a B.

A group examination of the rail pieces was conducted on February 20 and 21, 2013, at the NTSB Materials Laboratory in Washington, DC. Participants included representatives of the Federal Railroad Administration, CSX Transportation, the Brotherhood of Maintenance of Way Employees, and Sperry.

The pieces are shown in figure 1 in their relative positions based on the rail reconstruction. Mating fractures for the east end of piece N1, both ends of piece N5, and the west ends of pieces N15A and B were not observed in the recovered pieces. The remaining fractures all had mating sides. The west end of piece N1 was a cut end that was part of a rail joint that was found intact after the accident and was disassembled on-scene. The east end of piece N20 was cut on-scene after the accident to facilitate shipping and examination of the west end of piece N20. No weld joints were observed in the submitted pieces. The joint bars in piece N19B had been applied to repair a defect detected during an internal rail inspection conducted in July, 2012.

The rail pieces had raised stencil marks which read “136-10 CC BETH STEELTON 1997 IIIIII”, indicating that the rail size was 136 pound rail¹ manufactured in July, 1997. The raised markings were on the gage side of the web. The stencil was repeated along the length of the rail, and no different stencil marks were observed on any of the rail pieces.

The length of each piece that included a portion of the rail head was measured at the running surface. The measured distances were measured from fracture face to fracture face at the middle of the running surface, and in cases where the rail received end batter, the length of the piece was estimated using the mating side of the fracture as a guide to include the portion missing due to rail end batter in the total length measurement of that piece. In cases where the mating fracture surface was missing, the reported length is the longest distance at the running surface. Results of these measurements are listed in table 1.

Table 1. Length of Rail Pieces

Rail Piece	Length (inches)
N1	88.75
Missing length*	5
N5	20.25
N15B	6.625
N16B	9.25
N17B	11.125
N18	40.75**
N19B (west end to break within joint bars)	25
Total of above pieces	206.75

*The missing length between N1 and N5 was determined based on the missing length within the identification stencil on pieces N1 and N5.

**Length includes missing material due to end batter at the west end as determined using the mating fracture on piece N17B.

The fracture between N1 and N5 occurred through the raised stencil markings. On piece N1, the east fracture occurred through the east vertical leg of the “N” in “STEELTON”, and on piece N5, the fracture occurred approximately 0.44 inch east of the west tip of the “7” in “1997”. On a different intact area of the rail where the stencil was repeated, the distance between the “N” and “7” measured 5.44 inches. As a result, it was estimated that approximately 5 inches were missing between N1 and N5 as listed in table 1.

The total length of the rail between the cut end of piece N1 and the repaired defect was compared to measurements taken from internal rail inspection data obtained

¹ In the rail industry, rail size is referenced in pounds, which is the weight of a 3-foot length of rail.

from tests conducted in July, 2012, and August, 2012. Based on that data, it was estimated that the total length of rail from the west end of piece N1 to the location of the repaired defect in N19 was approximately 17 feet 1 inch (205 inches).

1. Hand Ultrasonic Inspection

A hand ultrasonic inspection of the rail pieces was conducted by a representative from Sperry participating in the examination. The rail was tested from the running surface using an Epoch Ultrasonic test unit with a 70-degree transducer. Each piece of rail with a rail head was scanned. No indications of internal defects were detected as a result of the hand inspection.

2. Rail Surface Condition

Views of typical features observed on the running surface of the rail are shown in figure 2. Surface cracks associated with rolling contact deformation were observed on the gage side of the running surface. Unlabeled arrows in the upper image in figure 2 indicate many of these surface crack features. Head checks² were generally observed at the gage corner of the head as shown in the lower image in figure 2.

3. Fracture Features

Views of the fracture surface at the east end of rail piece N1 are shown in figure 3. The upper and gage sides of the head were deformed and curled over the fracture surface consistent with trailing rail end deformation.³ A dark area with relatively flat fracture features and a smooth curving boundary was observed at the gage side of the head, features consistent with a transverse detail fracture.⁴ A dashed line in the upper image in figure 3 indicates the boundary of the detail fracture. The origin area of the detail fracture was obliterated by the trailing rail end deformation, but the shape of the boundary was consistent with a detail fracture emanating from the gage corner area. The size of the detail fracture covered approximately 9 percent of the remaining head area.

Fracture surfaces at the west and east ends of piece N5 are shown in figures 4 and 5, respectively. The head area including the gage corner of both pieces had post-fracture damage that obscured many of the fracture features. However, areas of dark oxide were observed on both pieces and portions of curving crack arrest boundaries were observed, consistent with transverse detail fractures at each end of piece N5. Dashed lines in the upper images in figures 4 and 5 indicate the approximate boundaries of the detail fractures. The fracture surface within the detail fracture at the west end of piece N5 appeared relatively rough near the boundary, consistent with

² Head checks are a rail surface condition where horizontal crack form in the deformation zone near the surface of the rail head. Where the cracks intersect the surface, they may form a saw-tooth or check-shaped pattern.

³ Trailing rail end deformation is deformation at the vertical face of the delivering rail end. It can occur when a misalignment or gap between the two rails allows the wheel to drop below the surface of the delivering rail.

⁴ In the rail industry, a fatigue crack at the gage side of the head is called a transverse detail fracture.

relatively rapid crack growth. Both fracture surfaces showed rubbing damage at the upper portion of the head fracture, and some receiving rail end deformation⁵ was observed at the running surface at the west end of piece N5. The overstress portions of the fractures at both the east and west ends of piece N5 appeared rubbed consistent with fracture surface recontact in the overstress regions. The transverse defects covered approximately 24 percent of the remaining head at the west end of piece N5 and 10 percent of the remaining head area at the east end of piece N5.

The fracture at the west end of piece N15B was angled between the transverse and horizontal planes. The fracture had uniform rough features consistent with overstress fracture. No evidence of a preexisting crack was observed, and no rail end deformation was observed. The fracture at the east end of piece N15B is shown in figure 6. A transverse detail fracture was observed in the gage corner as shown in figure 6, where the curving boundary of the detail fracture is indicated with a dashed line. The detail fracture covered approximately 2 percent of the remaining head area. The field side of the fracture was covered with reddish brown dirt.

The west end of piece N16B had fracture features that mated to the east end of piece N15B. The face of piece N16B was deformed consistent with receiving rail end batter.⁶ The fracture surface at the east end of N16B had a head check crack that appeared to be turning into the transverse plane. The transverse portion of the crack covered less than 1 percent of the remaining head area.

The fracture at the west end of piece N17B mated to the fracture at the east end of piece N16B. Some receiving rail end batter was observed at the west end of piece N17B. The east end of piece N17B had uniform rough features consistent with overstress fracture.

The west end of piece N18 mated to the east end of piece N17B, as determined largely by mating fracture features observed in the web and in the base (piece N17A). The head at the west end of piece N18 showed heavy receiving rail end batter, and wheel flange contact marks were observed on the web and base.

The fracture at the east end of piece N18 is shown in figure 7. An open head check was observed in the gage corner, and the start of transverse detail fracture growth from the area of the open head check was observed. A dashed line in figure 7 indicates the area of the open head check and transverse detail fracture growth. The size of the detail fracture was approximately 1 percent of the remaining head area (including the area of the open head check). The field side of the fracture was covered with reddish brown dirt.

⁵ Receiving rail end deformation is a deformation at the running surface associated with a gap in the rail where the wheel contacts the receiving rail which is located at the side of the gap in the direction of travel.

⁶ Receiving rail end batter is an impact deformation on the vertical face of a receiving rail end. It can occur when a misalignment or gap between two rails allows the wheel to drop below the surface of the delivering rail, and hammer against the end of the receiving rail as it rolls over the end corner of the rail.

The west end of piece N19 mated to the east end of piece N18. The fracture surface was covered with dirt and showed post-fracture damage. Evidence of flange contact was observed on the upper surface of the joint bar on the gage side of piece N19. The fracture at the east end of piece N19 mated to the fracture at the west end of piece N20 shown in figure 8.

A portion of the fracture surface at the west end of piece N20 had features consistent with a detail fracture as shown in figure 8. A dashed line in figure 8 indicates the boundary of the detail fracture. Receiving rail end deformation was observed at the running surface and gage corner at the upper side of the head, and the origin area of the detail fracture was obliterated by the receiving rail end deformation. However, the mating side of the fracture at the east end of piece N19 showed the detail fracture emanated from an origin at an open head check at the gage corner. The detail fracture covered approximately 15 percent of the remaining head area.

The joint in piece N19 was partially disassembled to facilitate examination of the fracture surfaces. The two bolts east of the repaired defect were removed, and the remaining two bolts were loosened, allowing the east portion of piece N19 to be removed from the joint bars. A view of the fracture surface with the repaired defect is shown in figure 9. A dashed line in figure 9 indicates the boundary of a detail fracture observed on the fracture surface. The detail fracture covered 73 percent of the remaining head area and extended out of the head into the web. The detail fracture originated at an open head check at the gage corner of the head.

4. Rail Cross-Section Measurements

Three transverse cuts were made in piece N5. Two of the cuts were made approximately 1 inch away from the fracture surfaces at each end of the piece. The third cut was made parallel to the cut near the west end to produce a 1-inch thick cross-section. A view of the transverse cross-section after cutting is shown in figure 10. For reference, an outline representing the cross-section of a new 136-pound rail is also shown in figure 10. The remaining head area was measured in the image shown in figure 10 and compared to the head area of the new 136-pound rail. The remaining head area in the accident rail represented 57 percent of the new head area, which corresponds to a 43 percent head loss.

The rail height, as measured at the middle of the running surface, was 6.793 inches on the pieces cut from piece N5. The height of a new 136-pound rail is 7.313 inches. By calculation, the vertical head loss for the accident rail was 0.520 inches. According to CSX engineering requirements for main track, 136-pound rail is to be scheduled for removal when the vertical head loss has reached 0.625 inch. The engineering requirements list a minimum rail height (wear limit) of 6.688 inches.

The width of the head was measured at a location 0.63 inches below the running surface. The head width at that location was 2.320 inches. The head width for new 136-pound rail is 2.938 inches. By calculation, the gage side wear for the accident rail was 0.618 inch. According to CSX engineering requirements for main track, 136-pound

rail is to be scheduled for removal when the side wear has reached 0.625 inch as measured at 0.63 inches below the running surface. The engineering requirements list a minimum rail head width (wear limit) of 2.313 inches.

5. Sizing of Detail Fractures

In the rail industry, detail defects are sized relative to the head area of a new piece of rail. However, defects sizes reported earlier in this report were sized relative to the remaining head area. Based on measurements showing the remaining head area of piece N5 was 57 percent of the head area of new 136-pound rail, the defect sizes of the transverse detail fractures were calculated relative to the original head area, and results are listed in table 2.

Table 2. Summary of Defect Size Measurements

Fracture Surface	Defect Size Relative to Remaining Head Area (percent)	Defect Size Relative to Original Head Area (percent)
N1 east end	9	5
N5 west end	24	14
N5 east end	10	6
N15 east end/N16 west end	2	1
N16 east end/N17 west end	<1	<1
N18 east end/N19 west end	1	<1
N19 east end/N20 west end	15	9

6. Metallography and Hardness

The rail cross-section removed from piece N5 (the piece shown in figure 10) was cut below the head to remove the head portion from the rest of the piece. Then the head portion was polished and etched with Nital, and the result is shown in figure 11. The microstructure observed on the polished and etched cross-section was pearlite, consistent with standard rail steel. Cracks were observed emanating from the surface at the gage corner and at the gage side of the running surface as indicated with unlabeled arrows in figure 11. These cracks were associated with the head checking and surface rolling contact deformation.

Hardness was conducted on the polished and etched cross-section of the head shown in figure 11. According to the 1997 AREMA specifications for standard rail steel,⁷ hardness was to be measured at 7 points on the rail head. Three of the points were located 0.375 inch vertically from the top center and 0.375 inch diagonally from the field and gage corner surfaces of a new rail head. The remaining four points were located 0.125 inch from the vertical sides of the head with two on the field side and two on the gage side. On each side, the lower point was located 0.125 inch above the lower

⁷ Manual of Railway Engineering, Chapter 4, Rail, American Railway Engineering and Maintenance-of-Way Association, Lanham, Maryland (1997).

surface of the head, and the other was located 0.875 inch below the top of the rail. All specified locations for hardness except the two points at 0.125 inch away from the field side of the head were missing due to wear on the accident rail head. Hardness was measured at the two locations specified for the field side of the head. The upper point was located relative to the original head surface, accounting for wear in the accident piece. The hardness of the upper point was 23.2 HRC. The hardness at the lower point was 28.5 HRC. Three additional hardness measurements were conducted between the upper and lower points at approximately 0.125 inches from the field side, and hardness measured at those points were 30.6 HRC, 31.2 HRC, and 30.2 HRC. The average of the 5 hardness measurements was 28.7 HRC. According to the 1997 AREMA specifications, the minimum specified tensile strength for standard rail steel was 140,000 pounds per square inch, which corresponds to an approximate hardness of 31 HRC.

Knoop hardness measurements were also conducted on the head along traces spanning from the field and gage corners and vertically from the surface to a point where the lower end of the head intersected the web centerline (see figure 11). A chart showing the Knoop hardness readings is presented in figure 12. The chart shows a general trend of decreasing hardness from adjacent to the rail head surface to the middle of the head. Near the surface, hardness measured 35 HRC (350 HK). Near the point where the head met the web centerline, hardness values measured with the Knoop test machine corresponded to a Rockwell hardness of 23 HRC.

7. Laser-Scanned Model of Piece N5

The remaining portion of piece N5 (after the ends were cut off) was scanned using a Faro QUANTUM FaroArm coordinate measurement device fitted with a Faro Laser ScanArm.⁸ A cloud of data points representing the surface of the rail piece was collected using Geomagic Studio software.⁹ The data was processed by making the point spacing uniform with a target number of points set at 3 million points. Next, the bottom plane was defined based on points collected from the table upon which the scanned piece was sitting, and the points collected from the table were removed. Then surfaces with 4 million triangles were created from the points. Next, a surface representing the bottom of the rail was created in the plane of the table and merged with the rest of the model. Then holes were filled using a curvature fill. Most of the holes were in the fillet area at the gage side of the rail and in the radius between the side of the base and the flat surface created to represent the rail bottom. The ends of the scanned piece were trimmed flat in the transverse plane, and the resulting openings at the ends of the piece were filled flat. Finally, the model was oriented with the positive X axis aligned along the rail to the east and the positive Z axis aligned with the up direction. An image of the resulting model of piece N5 is shown in figure 13, and a 3-dimensional portable document file (3D PDF) model is included in the electronic copy of

⁸ FARO Technologies, Inc., Lake Mary, Florida.

⁹ Geomagic, Morrisville, North Carolina.

this report as Appendix A.¹⁰ Arrows in figure 13 indicate marks observed on the base of piece N5 corresponding to contact locations for rail anchors.

Matthew R. Fox
Senior Materials Engineer

¹⁰ Adobe Reader 9 or later software is required to view 3D PDF files.

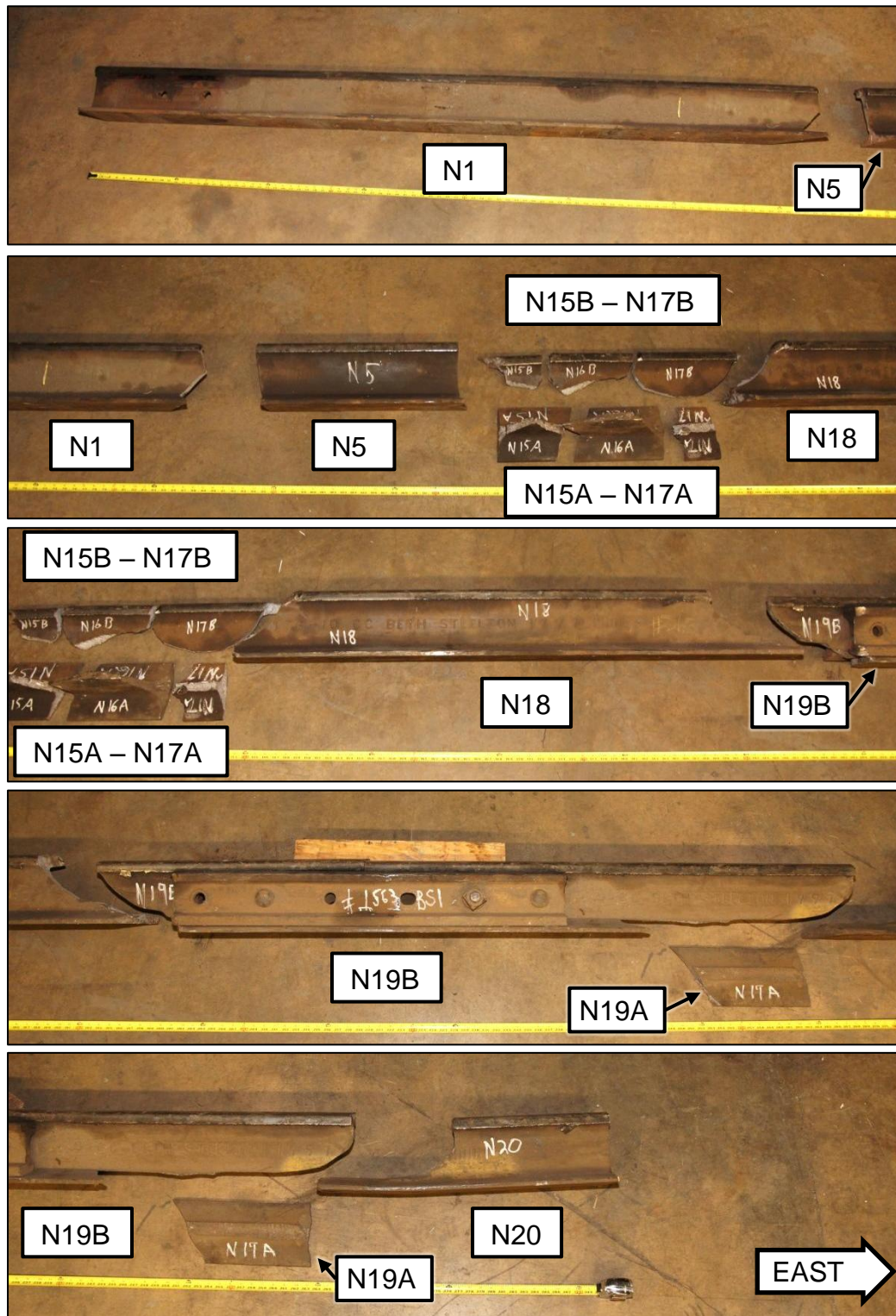


Figure 1. Overall views of the gage side of the submitted rail pieces.

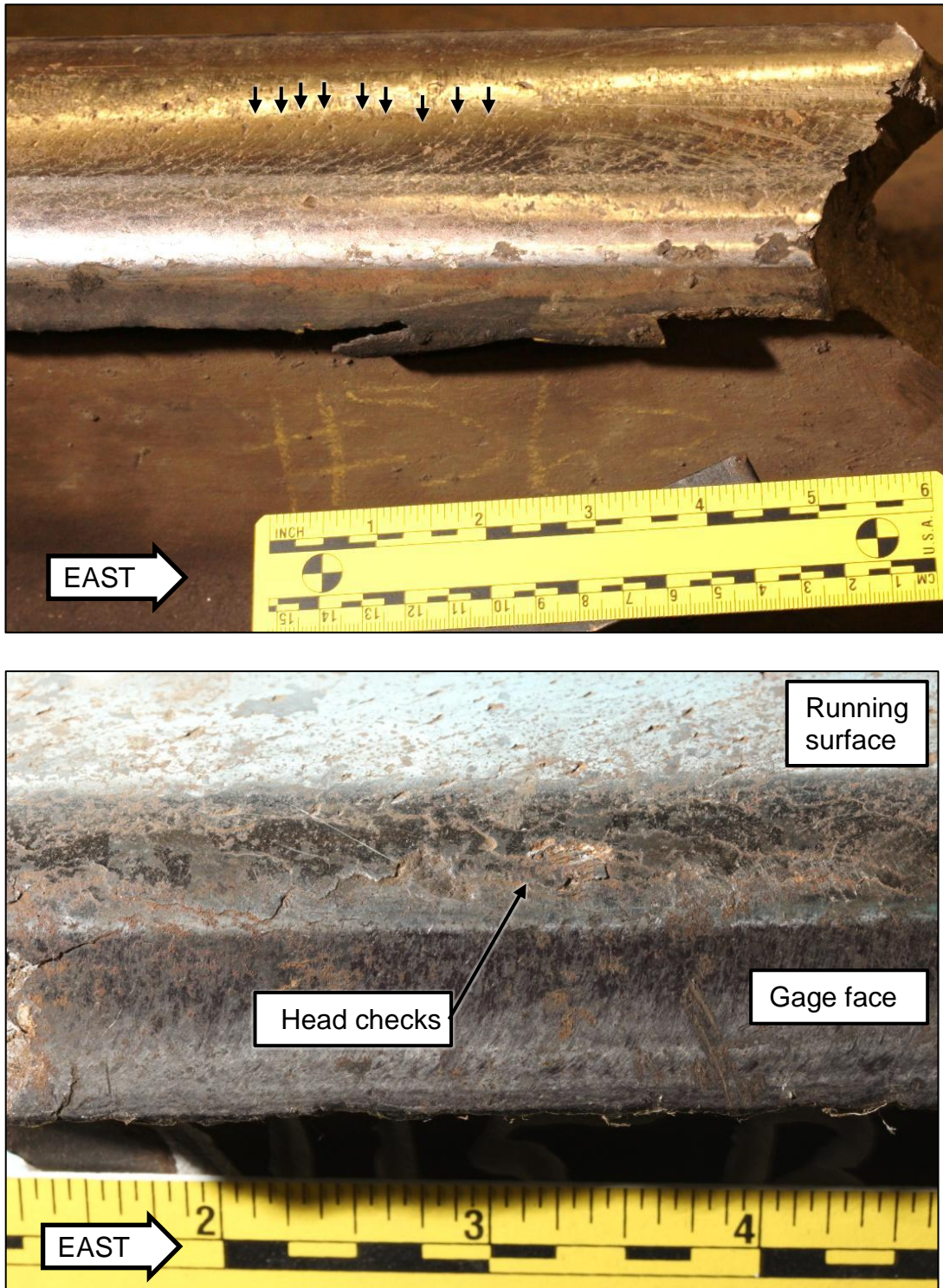


Figure 2. Views of the rail surface on two of the pieces showing rail surface conditions observed on the rail pieces. Unlabeled arrows in the upper image point to some of the cracks associated with surface rolling contact deformation as observed on the running surface near the gage corner.



Figure 3. Views of the fracture surface at the east end of piece N1. A dashed line in the closer view of the head indicates the boundary of a detail fracture emanating from the gage corner.

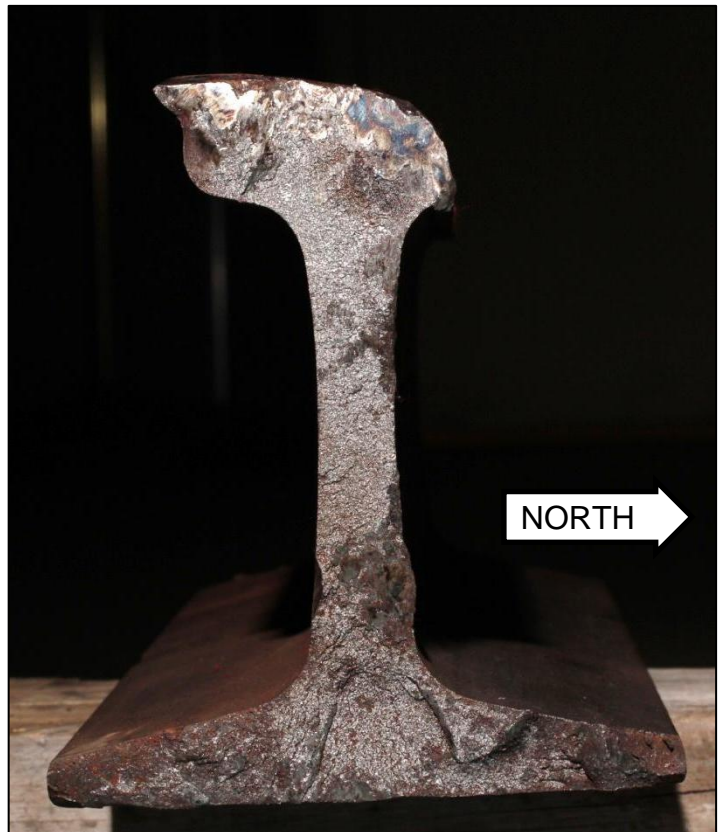


Figure 4. Views of the fracture surface at the west end of piece N5. A dashed line in the closer view of the head indicates the boundary of a detail fracture emanating from the gage corner.



Figure 5. Views of the fracture surface at the east end of piece N5. A dashed line in the closer view of the head indicates the boundary of a detail fracture emanating from the gage corner.



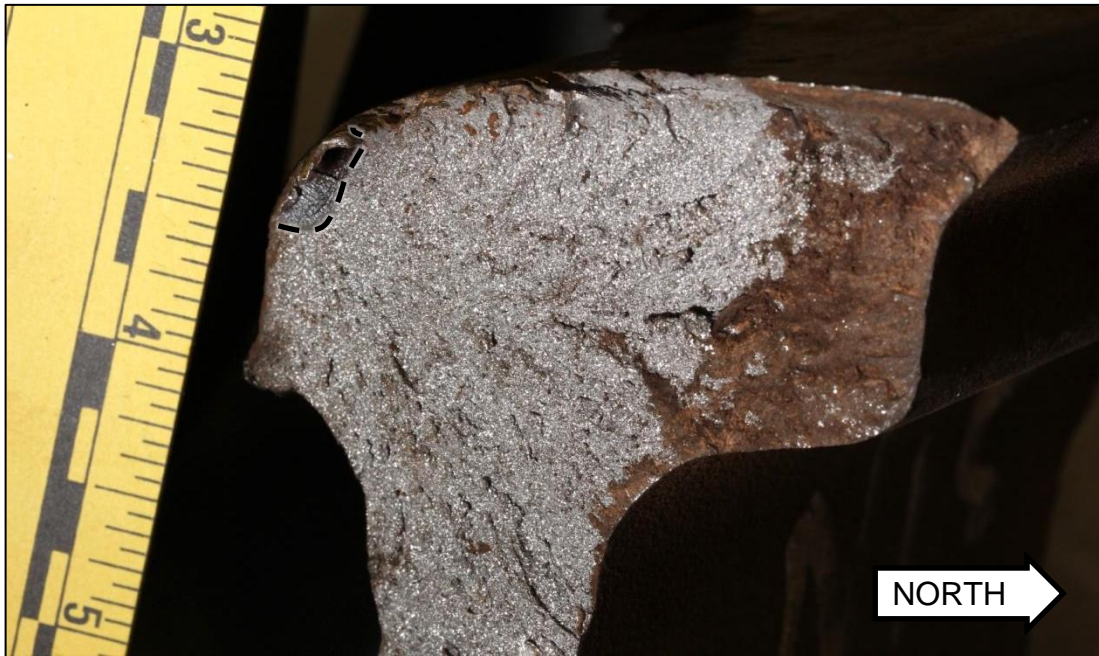


Figure 6. View of the fracture surface at the east end of piece N15B. A dashed line indicates the boundary of a detail fracture emanating from the gage corner.



Figure 7. View of the fracture surface at the east end of piece N18. A dashed line indicates the boundary of a detail fracture emanating from an open head check at the gage corner.



Figure 8. View of the fracture surface at the west end of piece N20. A dashed line indicates the boundary of a detail fracture emanating from the gage corner.



Figure 9. View of the fracture surface of the repaired defect in piece N19 after the joint bars were removed. A dashed line indicates the boundary of a detail fracture emanating from the gage corner.

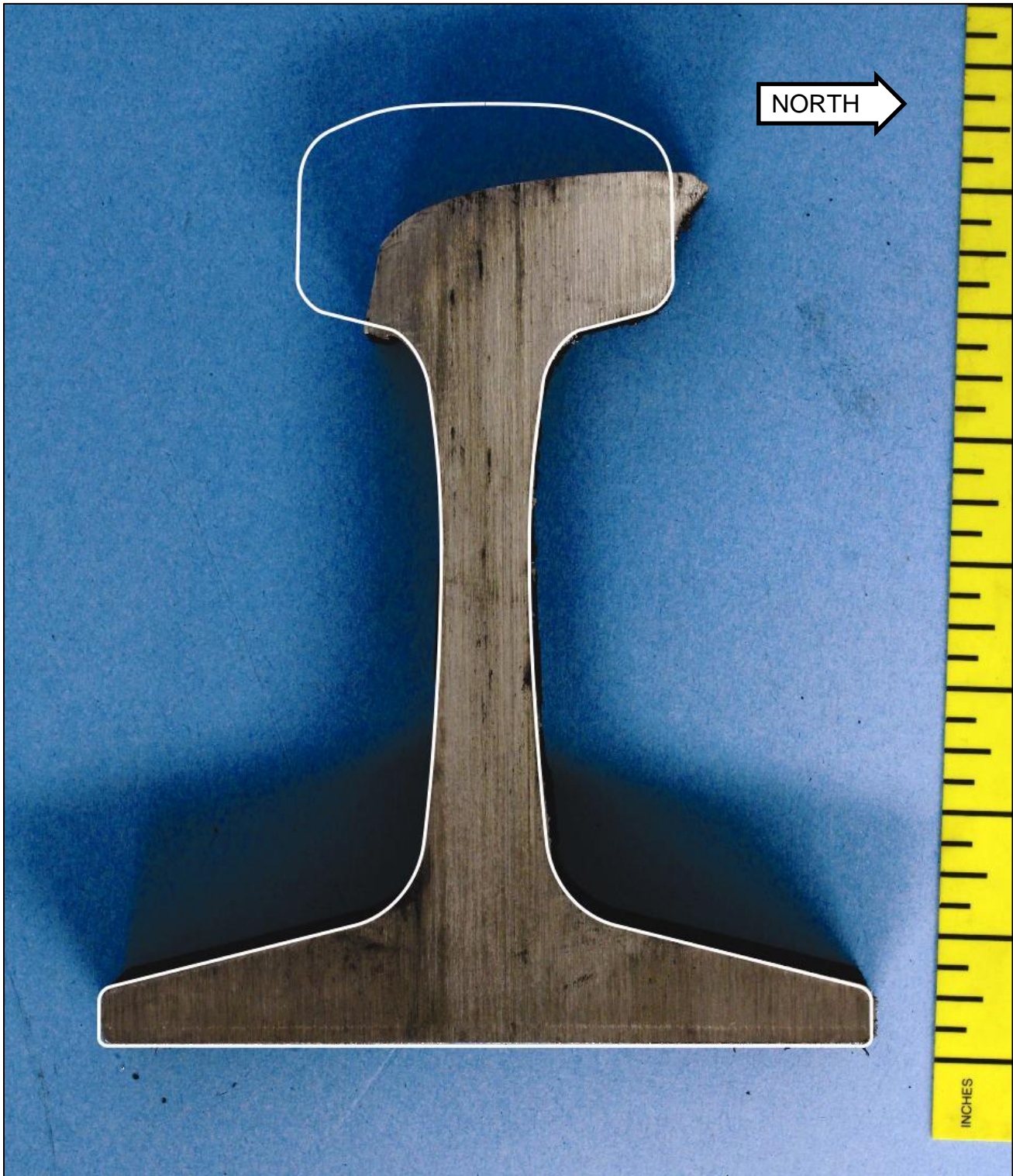


Figure 10. View of the rail cross-section (as-cut surface) near the west end of piece N5. The outline represents the cross-section of a new 136 pound rail.

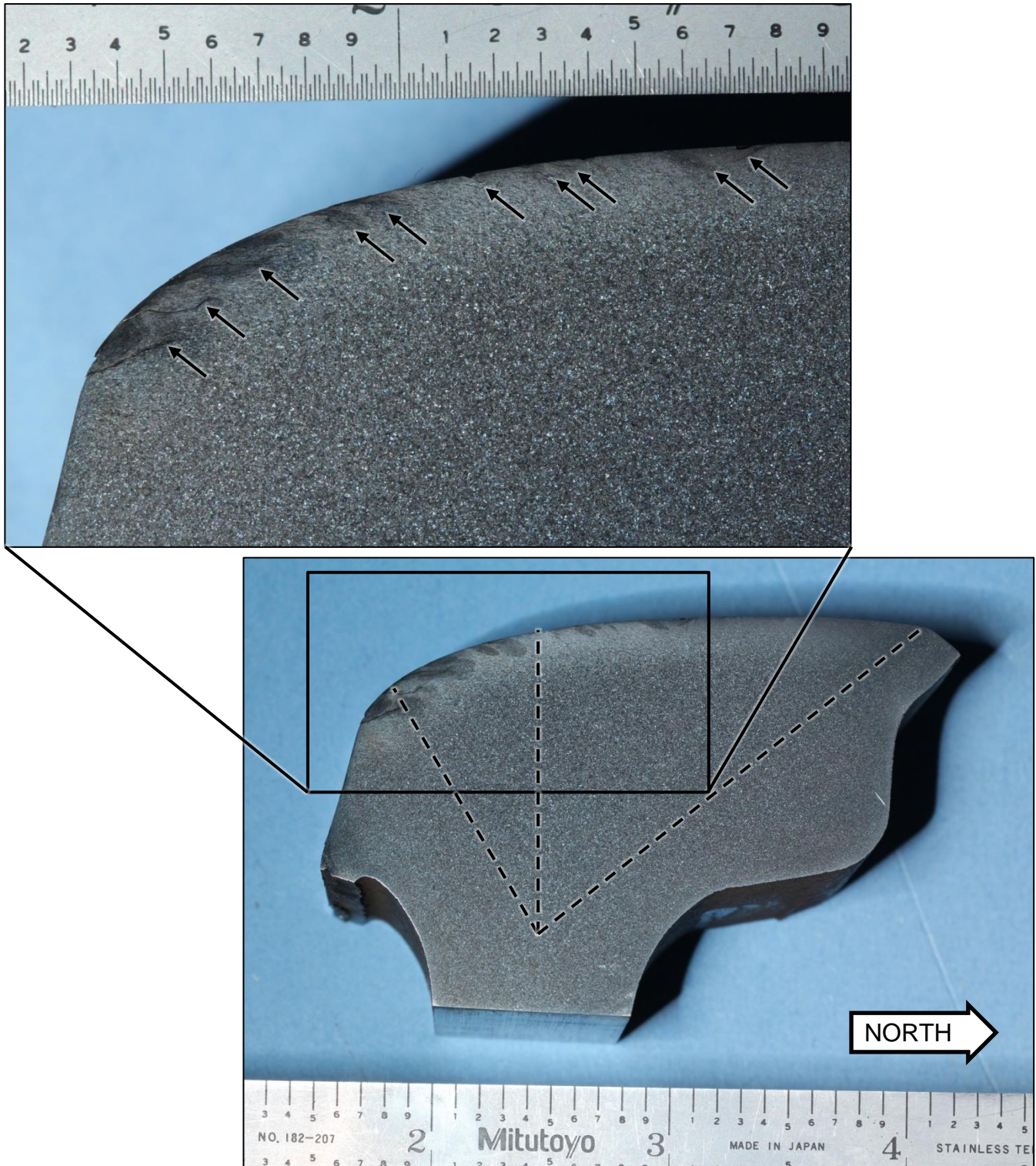


Figure 11. Views of polished and etched cross-sections of the head piece sectioned from rail piece N5. Arrows in the detail image indicate small cracks associated with head checks and surface rolling contact deformation. Dashed lines indicate locations of Knoop hardness traces conducted on the head.

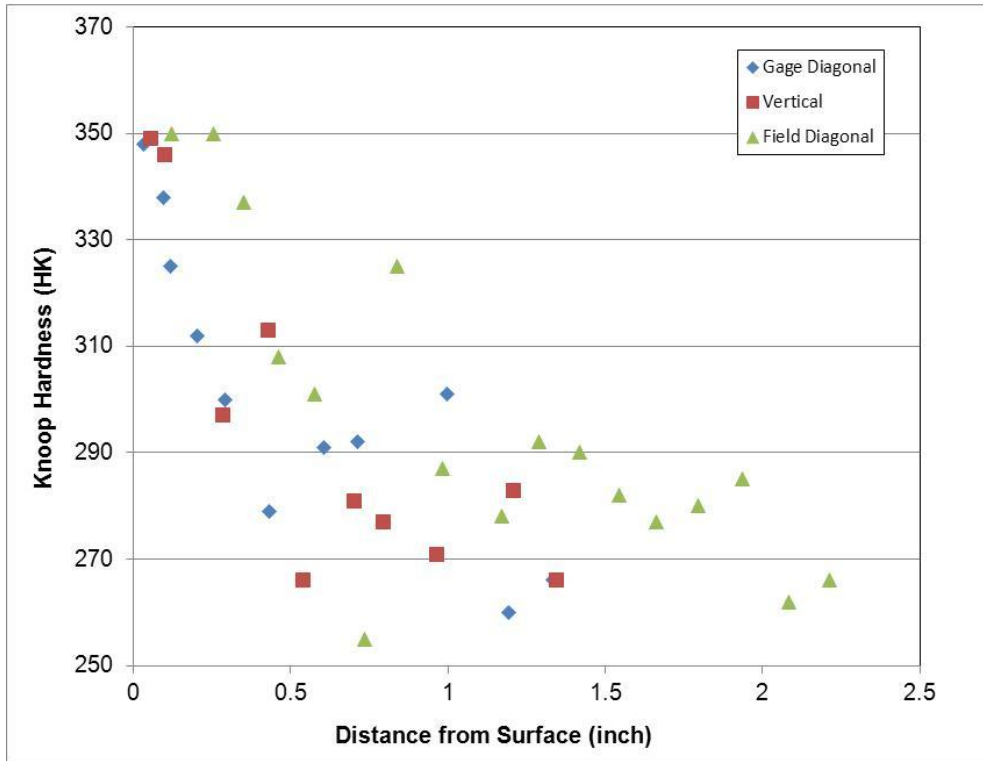


Figure 12. Chart showing Knoop hardness measurements measured along lines shown in figure 10.

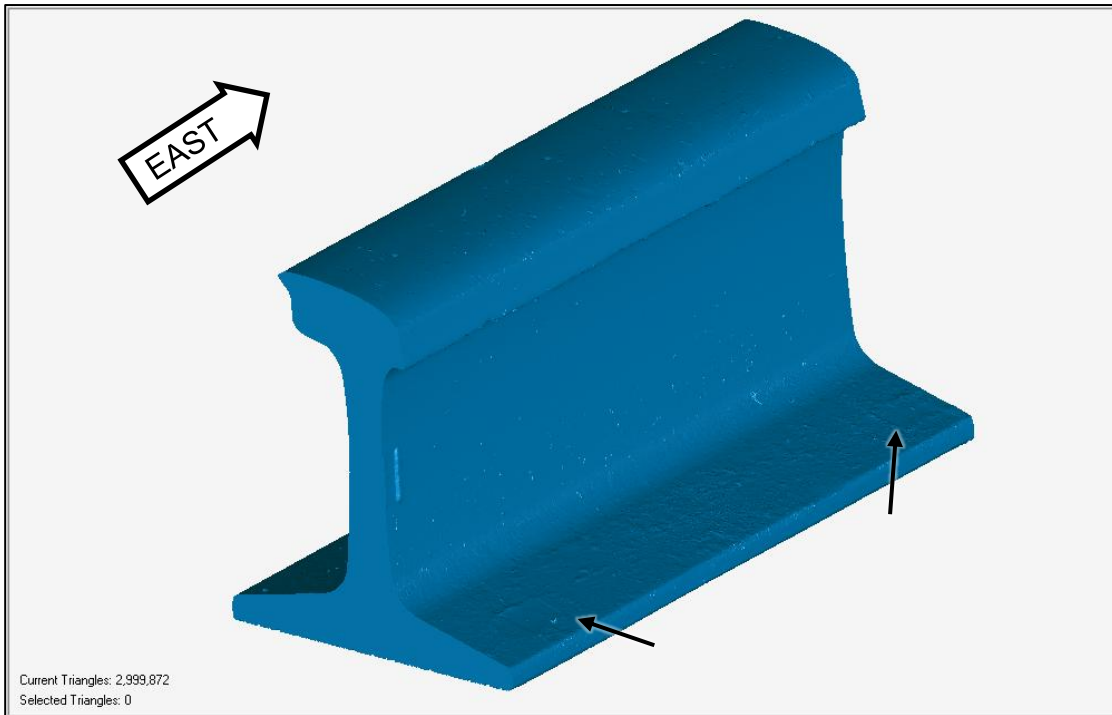
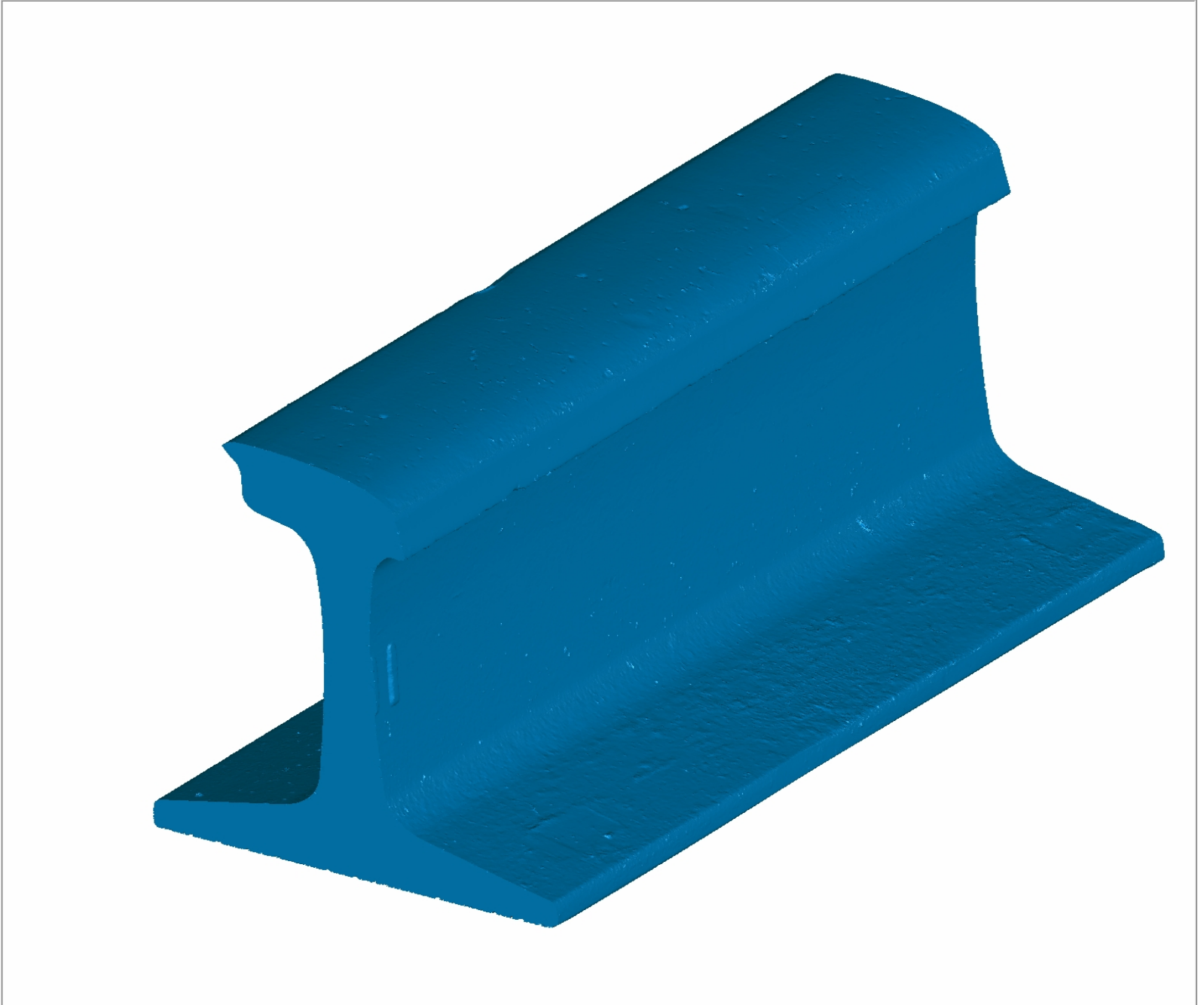


Figure 13. Laser scan representation of the piece N5 after fractured ends and a transverse cross-section piece were cut from the ends. Arrows indicate location of anchor contact marks on the base.

D. APPENDIX A. 3D PDF OF SCANNED RAIL

geomagic



Click on the image to activate the 3D Model.